Clinical EEG and Neuroscience
2015, Vol. 46(3) 183–191

DOI: 10.1177/1550059414523959
eeg.sagepub.com
SAGE

Small-World Brain Functional Networks in Children With Attention-Deficit/Hyperactivity Disorder Revealed by EEG Synchrony

Tian Liu[1,2], Yanni Chen[1,2,3], Pan Lin[1,2], and Jue Wang[1,2]

Abstract

We investigated the topologic properties of human brain attention-related functional networks associated with Multi-Source Interference Task (MSIT) performance using electroencephalography (EEG). Data were obtained from 13 children diagnosed with attention-deficit/hyperactivity disorder (ADHD) and 13 normal control children. Functional connectivity between all pairwise combinations of EEG channels was established by calculating synchronization likelihood (SL). The cluster coefficients and path lengths were computed as a function of degree *K*. The results showed that brain attention functional networks of normal control subjects had efficient small-world topologic properties, whereas these topologic properties were altered in ADHD. In particular, increased local characteristics combined with decreased global characteristics in ADHD led to a disorder-related shift of the network topologic structure toward ordered networks. These findings are consistent with a hypothesis of dysfunctional segregation and integration of the brain in ADHD, and enhance our understanding of the underlying pathophysiologic mechanism of this illness.

Keywords

ADHD, EEG, graph theory, small-world networks, Multi-Source Interference Task

Received June 6, 2013; revised January 4, 2014; accepted January 15, 2014.

Introduction

Children with ADHD are generally inattentive, impulsive, and hyperactive.[1] It is estimated that about 5% to 8% of children worldwide have ADHD. It is one of the most common childhood neurobehavioral disorders, which frequently persists into adolescence and adulthood.[2]

Many neuroanatomic and neuropsychological studies have shown that the symptoms of ADHD may be related to anatomic[3,4] and functional[5,6] connectivity abnormalities involving some interacting neural regions, such as the dorsal anterior midcingulate cortex, dorsolateral prefrontal cortex, ventrolateral prefrontal cortex, parietal cortex, striatum, and cerebellum. These regions mainly constitute attention and cognition parallel networks.[1] Research into the brain-defect theory of ADHD is increasingly focusing on disorders in the brain network.

Recent advances in graph theoretical approaches have allowed researchers to characterize topologic properties of complex brain networks. In 1998, Watts and Strogatz[7] showed that graphs with many local connections, and a few random long-distance connections, defined as "small-world networks," were representative of near-optimum structure networks, which should be simultaneously well segregated (local feature) and integrated (global feature). Since then, the study of complex networks has become a hot topic in the field of neurology.[8] Several recent studies have demonstrated that the small-world properties of brain networks are affected by brain diseases, such as spinal cord injury,[9] Alzheimer disease,[10] epilepsy,[11] schizophrenia,[12] and brain tumor.[13] There is also some evidence that ADHD is associated with brain functional network abnormalities.[14,15] However, to date, little is known about the small-world topologic organization of brain attention functional networks in ADHD. In the present study, we hypothesize that the topologic organization of brain attention functional networks is altered in children with ADHD.

[1]The Key Laboratory of Biomedical Information Engineering of Ministry of Education, Institute of Biomedical Engineering, School of Life Science and Technology, Xi'an Jiaotong University, Xi'an, China
[2]National Engineering Research Center of Health Care and Medical Devices, Xi'an Jiaotong University Branch, Xi'an, China
[3]Maternal and Child Health Hospital, Xi'an, China

Corresponding Author:
Jue Wang, Institute of Biomedical Engineering, Xi'an Jiaotong University, Xi'an 710049, China.
Email: juewang_xjtu@126.com
Full-color figures are available online at http://eeg.sagepub.com

To test this hypothesis, EEG was used to construct brain attention functional networks of children with ADHD and normal controls during performance of the MSIT. This task has been shown to effectively activate cognitive and attention networks.[16] In this study, we established a functional connectivity matrix, by calculating the SL[17] between all pairwise combinations of EEG channels during MSIT performance. The topologic properties of the graph were computed by graph theoretical analysis. Finally, the differences between the ADHD and control groups were statistically evaluated.

Materials and Methods

Subjects

The study included 13 outpatient boys diagnosed with ADHD (age range, 6–13 years; mean age, 8.5 ± 3.17 years; mean IQ score, 93 ± 16.8; all right handed) and 13 age-matched and gender-matched normal control children (age range, 6–13 years; mean age 7.9 ± 1.98 years; mean IQ score, 98 ± 18.3; all right handed). Written informed consent was obtained from all parents of the participants, according to the Declaration of Helsinki. The ethics committees of the Xi'an Jiaotong University School of Medicine approved the study. All participants had full-scale and verbal IQ scores > 80 (Wechsler Intelligence Scale for Children, Fourth Edition). All participants' parents filled out translated versions of the Conners' Parent Rating Scales–Revised[18] and the ADHD Rating Scale-IV for current and childhood-onset ADHD symptoms. The ADHD Rating Scale-IV is a reliable and easy-to-administer instrument both for diagnosing ADHD in children and adolescents and for assessing treatment response. The scale is linked directly to the diagnostic criteria for ADHD of the *Diagnostic and Statistical Manual of Mental Disorders*, Fourth Edition (*DSM*-IV).[19] Many researchers, such as van Dongen-Boomsma et al[20] and Lahey et al,[21] have used DSM-IV to diagnose ADHD. The ADHD Rating Scale-IV includes 2 parts: attention deficit and hyperactivity/impulsivity. The 2 parts each have 9 symptoms; if a symptom lasts > 6 months and does not fit with the developmental level, the symptom is valid. This scale contains 18 items (ADHD symptoms); 1 symptom represents 1 point. In the range of 1 to 18, the more symptoms, the higher the score. Subjects with higher *DSM*-IV scores have more serious ADHD. The *DSM*-IV scores of ADHD (mean, 13.23 ± 3.22) were significantly higher than controls (mean, 5.23 ± 2.09) ($P < .01$). An experienced child psychiatrist and health care psychologist made the diagnosis of childhood-onset, current, combined or inattention subtype. The criteria for ADHD included (1) endorsement of ≥6 of 9 *DSM*-IV symptoms of inattention, and ≥6 of 9 *DSM*-IV symptoms of hyperactivity/impulsivity; (2) no history of using stimulant medications, severe brain injuries, or other neuropsychiatric disorders; and (3) no evidence of cognitive deficit, learning disabilities, and communication problems as determined through clinical histories and parent interviews. Normal controls were excluded if they were diagnosed with ADHD and they had histories using stimulant medications, severe brain injuries, other neuropsychiatric disorders, cognitive deficit, learning disabilities, and communication problems.

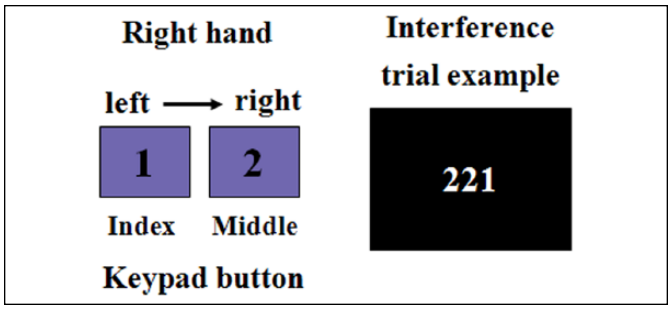

Figure 1. Illustration of the MSIT. During the interference trials, subjects pressed the button to identify the number that differed from the other 2 numbers (Flanker stimuli), and the targets never matched the button location (Stroop effect). In this example, the 1 is different from the 2 numbers, so the correct answer would be to press button 1.

Task Description

The MSIT, which combines multiple dimensions of cognitive interference in a single task, is known to activate a network of brain regions involved in attention and cognitive control.[16] Subjects were given a button-press and informed that the left and right keypad buttons represented 1 and 2, respectively. They were instructed to use the index and middle fingers of their right hands to respond (Figure 1, left). In the present study, the MSIT included only interference trials. The total set of possible interference stimuli is 112, 212, 221, and 211. An example of the stimuli in a single trial is shown on the right side of Figure 1. During interference trials, distractors were drawn from a set of potential target numbers (1, 2); target numbers were never placed congruently with their button box positions (Stroop effect[22]), and the Flanker stimuli[23] were always potential targets. Subjects were asked to report the identity of the digit that differentiated the other 2 numbers by pressing the appropriate button. Before the start of the experiment, each subject underwent some adaptive exercises. All interference trials would appear at the center of the screen every 3 seconds, with 15 seconds of fixation (a white dot in the center of the screen). During fixation, subjects completed 80 random trials.

EEG Recordings

EEGs were recorded from 19 electrodes at the following scalp locations of the 10-20 system: FP1, FP2, F3, F4, F7, F8, Fz, T3, T4, T7, T8, C3, C4, Cz, P3, P4, Pz, O1, and O2 (Neuroscan; Compumedics Limited, Charlotte, NC). Electrode impedance was <5 kΩ. The reference electrode was at the left mastoid, and the ground electrode was between FPz and Fz. A vertical electro-oculogram was recorded from electrodes attached above and below the left eye, and a horizontal electro-oculogram was recorded from the outer canthi of both eyes. EEG was sampled with 32 bits of accuracy, and the analog/digital sampling rate was 1,000 Hz. All participants were seated inside an acoustically and electromagnetically shielded room. Participants were asked to minimize all movements during the experiments.

EEG Preprocessing

Because the average reaction times (RTs) of the 2 groups on the MSIT were 1,703 ± 522 and 1,162 ± 462 ms, all subjects were able to react to the task in about 2 seconds, so we defined the period from target stimulus onset to 2 seconds as the response period. Only correct trials were segmented, and each subject had 10 epochs (total, 20 seconds; 20,000 samples) of artifact-free data (no ocular and muscular artifacts). Wavelet packet analysis was performed on every EEG data segment,[24] and EEG components of the following 4 frequency bands were obtained: delta (0.5–3 Hz), theta (4–7 Hz), alpha (8–13 Hz), and beta (13–30 Hz).

Computing SL

SL is based on the concept of general synchronization[17] between 2 time series, which takes account of both linear and nonlinear synchronization. The time series were reconstructed in a state space, according to Taken's theorem, by determining 2 characteristics: the time lag (L) and embedding dimension (M). The co-occurrence of neighboring states (similar patterns) was then quantified, which considers the degree of similarity between the states. The SL ranges between P_{ref} (a small number close to 0) and 1, with low SL indicating no synchronization and high SL representative of total synchronization. W_1 and W_2 were windowing parameters, where W_1 was the Theiler correction for autocorrelation, and W_2 was the improved time resolution of the synchronization measurement. L, M, P_{ref}, W_1, and W_2 were parameters that had to be set; in the present study, $L = 1$, $M = 10$, $P_{ref} = 0.01$, $W_1 = 100$, and $W_2 = 400$. SL was computed between each pair of electrodes, resulting in a square $N \times N$ matrix of size 19 (the number of EEG channels) per subject; the values on the diagonal were ignored. We computed the SL for the aforementioned 4 EEG bands.

Because 1 epoch, 2,000 samples (2 seconds), is short for calculating SL, we used 2 epochs (4 seconds, 4,000 samples) to generate SL and then calculated the average value of SL, which was standardized for each subject.

Graph Theoretical Analysis

An SL matrix of an undirected binary graph is a symmetric matrix. The SL matrix can be converted to a graph by considering a threshold T. Because there is no unique way to choose T, we explored a range of values for T. Through calculation, the average thresholds for the ADHD group and the control group were 0.064 and 0.052, respectively. As mentioned above, SL values range from 0.01 to 1, so we selected a threshold range of $0.01 < T < 0.05$ (in steps of 0.001) and then analyzed for each value. If the SL between a pair of channels i and j exceeds T, an edge is said to exist between i and j; otherwise no edge exists between them. After the SL matrix has been converted to a graph, the network parameters of interest are calculated for this model of a brain network, such as degree K, cluster coefficient C, and characteristic path length L. Definitions and computation of K, C, L are in the Appendix.

However, under a given threshold, the edges of the 2 graphs (ADHD and control) will also differ. This will influence the differences in C and L between the 2 groups. To control for this effect, we computed C and L as a function of degree K. The advantage of doing this is that network graphs in both groups contain the same number of edges, so that any remaining differences in C and L between the groups would reflect differences in network organization. Degree K was used as a variable to calculate the values of C and L and to compare with the theoretical values of C and L for ordered ($C = 3/4$, $L = N/2K$) and random ($C = K/N$, $L = \ln[N]/\ln[K]$) networks. For the range of $2 < K < 6$, with a step of 0.1, random, ordered, and real experimental networks were calculated. At each threshold T value or degree K value, there was one C, and L values were calculated per subject. Finally, we calculated the average C and L in the ADHD and normal control groups.

In general, statistical comparisons of networks need to have the same (or similar) degree sequences, because these will affect the network measurement. However, because the theoretical networks have Gaussian degree distributions, they may not provide an effective contrast for our experimental networks. To statistically compare the differences of C and L between the experimental networks (ADHD and control) and theoretical networks (ordered and random), we selected $K = 4$ to generate random and ordered networks, following the procedure described by Milo et al,[25] which preserves the degree distribution exactly. For $K = 4$, for each EEG, 15 random and 15 ordered networks were generated, and the mean C and L were calculated and then compared with the C and L of the experimental networks. Optimal networks, characterized by high C and low L, are designated small-world networks.[7]

Small-World Network Property

Small-world network property not only reflects the functional segregation (local) and integration (global) information exchange properties of the brain, it also reflects the adaptability of the human brain to various internal and external stimuli. For a small-world network, L should be close to a random network value ($\gamma = L^{real}/L^{rand} \approx 1$), and C should be much larger than the random network ($\gamma = C^{real}/C^{rand} >> 1$). These can be represented by a scalar, which is the small-world value ($\sigma = \gamma/\lambda$). When $\sigma > 1$, the network has a small-world property.

Statistical Analysis

SPSS version 13.0 (SPSS, Inc, Chicago, IL) was used for all statistical analyses. The Shapiro-Wilk test was used to test for normality of distribution. RT and accuracy were analyzed using a 2 groups (ADHD vs normal control) × 1 condition ($MSIT_{Interference}$) analysis of variance. C and L in terms of the differences between the ADHD group and the control group were compared using the Wilcoxon rank sum test. The Pearson test was performed to analyze the correlation between the EEG network feature (C and L) and clinical behavioral symptom or task performance. P values <.05 were considered to indicate statistical significance.

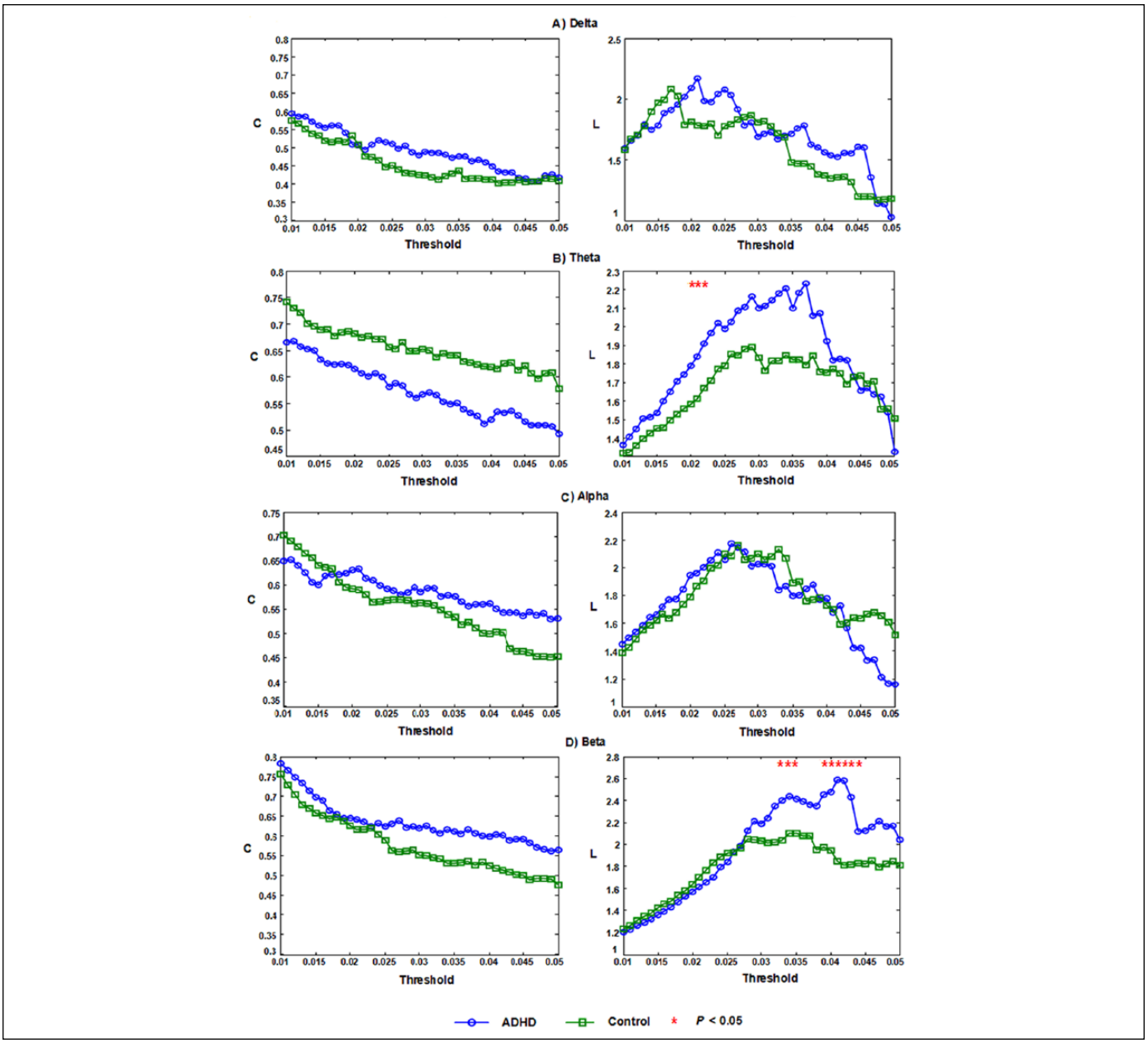

Figure 2. Mean clustering coefficient *C* and characteristic path length *L* for children with ADHD (circles) and normal controls (squares) as a function of threshold *T* in all EEG bands of interest. The asterisks indicate significant differences between the 2 groups ($P < .05$).

Results

The mean RTs for the ADHD and control groups were 1,703 ± 522 and 1,162 ± 462 ms. The mean levels of accuracy for the ADHD and control groups were 90.63 ± 0.1% and 93.75 ± 0.08%. In the interference trials, RTs were significantly longer for patients with ADHD than for normal controls ($F = 6.019$, $P = .025$). The accuracy of patients with ADHD was less than that of normal controls, but not significantly ($F = 1.358$, $P = .254$). Children who are diagnosed with ADHD are generally inattentive and hyperactive. In this study, participants were asked to minimize all movements during the experiments, and RTs were significantly longer for patients with ADHD than for normal controls. We thus inferred that this behavioral result, in which children with ADHD were slower to react during performance of the MSIT (compared with normal children), was likely related to the core clinical symptom of ADHD: inattention. We also found, at the beginning of the experiment task trials, that the 2 groups had no significant difference in RT, but as the experiment continued, the subjects with ADHD could not effectively focus their attention on the task, resulting in their increased response times to the task.

Figure 2 shows the mean clustering coefficient *C* and characteristic path length *L* as functions of the thresholds for the ADHD and control groups in the 4 EEG bands of interest. As expected, the connectivity between the vertices (EEG

channels) disappeared with increases in the threshold, and C was also seen to decrease. However, when the threshold was small, L increased linearly with increases in the threshold. As the threshold continued to increase, L tended to flatten. This is because for thresholds with high values, some vertices will lose their connections, and the shape of the graph will be smaller, limiting the growth of L. When the threshold increased to a certain extent, L decreased. This can be explained by the graph being divided into 2 or more subgraphs as the threshold increases; these subgraphs are smaller than the original graph, so L also decreases.

There were no significant differences between the 2 groups for C and L in delta and alpha bands (Figures 2A and 2C). In theta (Figure 2B), for the range of T (0.02–0.022), L was significantly larger for ADHD than normal controls ($P < .05$), and the most significant difference was found for $T = 0.022$ ($W_{ADHD} = 0.754$, $W_{con} = 0.858$; Wilcoxon rank sum test, $P = .0276$), but there was no significant difference in C for the 2 groups. In beta (Figure 2D), for the range of T (0.032–0.034 and 0.039–0.044), L was significantly larger for ADHD than controls ($P < .05$), and the most significant difference was found for $T = 0.041$ ($W_{ADHD} = 0.892$, $W_{con} = 0.774$; Wilcoxon rank sum test, $P = .0051$), although there was no significant difference in C for the 2 groups.

To control for the impact of 2 groups with different SL, we repeated the analysis computing C and L as a function of degree K. Figure 3 illustrates the mean C and L values computed in ADHD and controls as a function of K, for all frequency bands of interest. We found that the mean clustering coefficient of the real graphs of the 2 groups was enhanced, with an increase in degree K, and was intermediate between the theoretical ordered ($C = 3/4$, $L = N/2K$) and theoretical random ($C = K/N$, $L = \ln[N]/\ln[K]$) graphs. In addition, C was larger for ADHD than controls; the mean L of the 2 real graphs was smaller than the theoretical ordered and random graphs for $K < 3.5$.

In delta and theta (Figures 3A and 3B), there were no significant differences between the 2 groups for C and L. In alpha (Figure 3C) for the range of K (4.3–4.5), C was significantly larger for ADHD than controls ($P < .05$), but there was no significant difference in L for the 2 groups. In beta (Figure 3D), for the range of K (2.9–4.3), C was significantly larger for ADHD than the controls ($P < .05$). In addition, for the range of K (4–4.6), L was significantly greater for ADHD than controls ($P < .05$).

Because the beta rhythm was thought to relate to alertness, and as the activity of beta increased, the performance of the vigilance task also increased.[26] This research focused mainly on whether the attentional functional brain networks of children with ADHD would alter during MSIT performance. Moreover, we also found that C and L in the 2 groups were most significantly different in beta (Figure 3). Therefore, the present study mainly analyzed the brain function network characteristic of the beta band in the following.

For $K = 4$, a comparison was made of C and L of real experimental networks (ADHD and controls) with those of the constructed random and ordered networks, which had the same degree sequences as the real networks, in beta. As shown in Figure 4, C in the real network was intermediate between generated ordered and random networks, whereas L in the real was lower than L in generated ordered networks and close to L in the generated random networks. Moreover, C ($P = .0423$) and L ($P = .0417$) were both significantly larger for ADHD than normals ($W_{ADHD} = 0.812$, $W_{con} = 0.843$).

Small-world network property σ is a scalar, which is defined as: $\sigma = \gamma/\lambda$ ($\lambda = L^{real}/L^{rand}$ and $\gamma = C^{real}/C^{rand}$). We chose $K = 4$ to generate the random networks, then calculated the λ, γ, and σ values at $K = 4$ in beta. The small-world property values of ADHD and normals were $\sigma_{ADHD} = 1.55$ and $\sigma_{con} = 1.45$, which showed that both groups had economical small-world properties during performance of the MSIT in beta ($P = .14$).

Correlation analyses were conducted to assess relations between EEG network feature and clinical behavioral symptom or task performance in beta. As shown in Figure 5, we found that *DSM*-IV scores of all participants (both ADHD and normals) were positively correlated with cluster coefficient ($r = 0.575$, $P = .008$), but not for ADHD alone ($r = 0.354$, $P = .316$). *DSM*-IV score can reflect the level, with higher scores indicating more serious ADHD. *DSM*-IV scores of controls were low, and those of ADHD were high, and C in ADHD was significantly higher than in controls in beta. These results indicate that children with ADHD had more symptoms and higher values of C than controls. Therefore, the *DSM*-IV scores of all participants (both ADHD and controls) were significantly positively correlated with their C values, indicating that the more ADHD symptoms, the higher their cluster coefficient C. There was no significant correlation between path length and *DSM*-IV scores for the combined ADHD and control groups ($r = 0.153$, $P = .519$) or for the ADHD group alone ($r = -0.116$, $P = .750$).

In addition, as shown in Figure 6, we found that the correlation between RT and the cluster coefficient was significant for ADHD ($r = 0.885$, $P = .001$), but not for controls ($r = 0.414$, $P = .234$). No significant correlation was observed between RT and path length for ADHD ($r = -0.562$, $P = .091$) or the controls ($r = -0.414$, $P = .235$).

Discussion

We observed the small-world configuration in the brain attention function networks in children using EEGs recorded during performance of the MSIT. We found that both C and L were greater for ADHD than normals This indicates that the local feature was enhanced in ADHD, but the global characteristic was weaker.

The characteristic path length L plays an important role in the transmission of information in the network. It is a global characteristic that describes a network's internal structure and indicates how well integrated the network is (see the Appendix). Because L characterizes the average path of information from vertex i to all other vertices, smaller L values mean that a network can transmit information more quickly, and vice versa. It has been suggested that L is affected by the loss of long-range connections.[27] The findings of structural and diffusion imaging

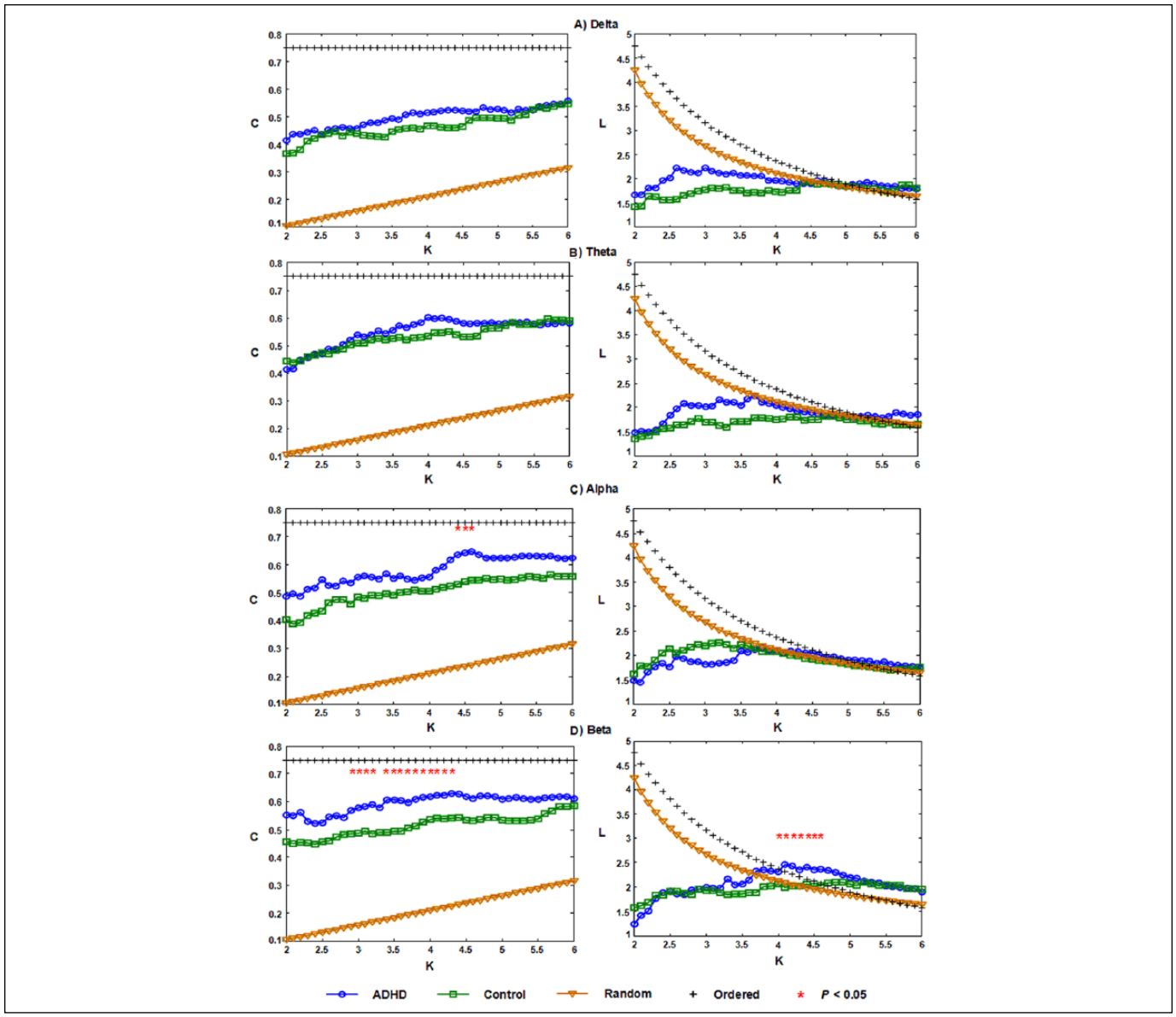

Figure 3. Mean clustering coefficient *C* and characteristic path length *L* as a function of the degree *K* in the brain graph. *C* and *L* for children with ADHD (circles) and normal controls (squares) were compared with the theoretical values of *C* and *L* for ordered (crosses) and random (triangles) networks as a function of degree *K* in all EEG bands of interest. Asterisks indicate significant differences between the 2 groups ($P < .05$).

studies have suggested that ADHD is related to the abnormality of long-range connections, which could interfere with the brain's long-range information exchange.[3,4] All these abnormalities may contribute to the tendency of *L* of the brain network to increase in ADHD. We found that *L* was significantly greater in ADHD than in normal children. This indicates that the global characteristic was weaker in ADHD, and that communication between different parts of the brain was more effective (information was transmitted more quickly) in normals than in ADHD during MSIT performance.

We also found that children with ADHD had increased local characteristics compared with normals. The underlying mechanisms of increased local characteristics have been widely discussed in relation to many diseases.[9,27] In this study, the fact that the local characteristics of the task-related network were enhanced in ADHD might reflect a compensatory mechanism to inhibit the impact of the disorder on the brain networks. Because there were problems with long-range communication in ADHD, there was a trend toward increased local short connections. These findings are consistent with the results of Wang et al.[14]

The brain is a complex network, and the small-world property is one of a number of important network properties. Although the ADHD group also had salient small-world properties ($\sigma_{ADHD} = 1.55 > 1$) in beta, this was due to the increased

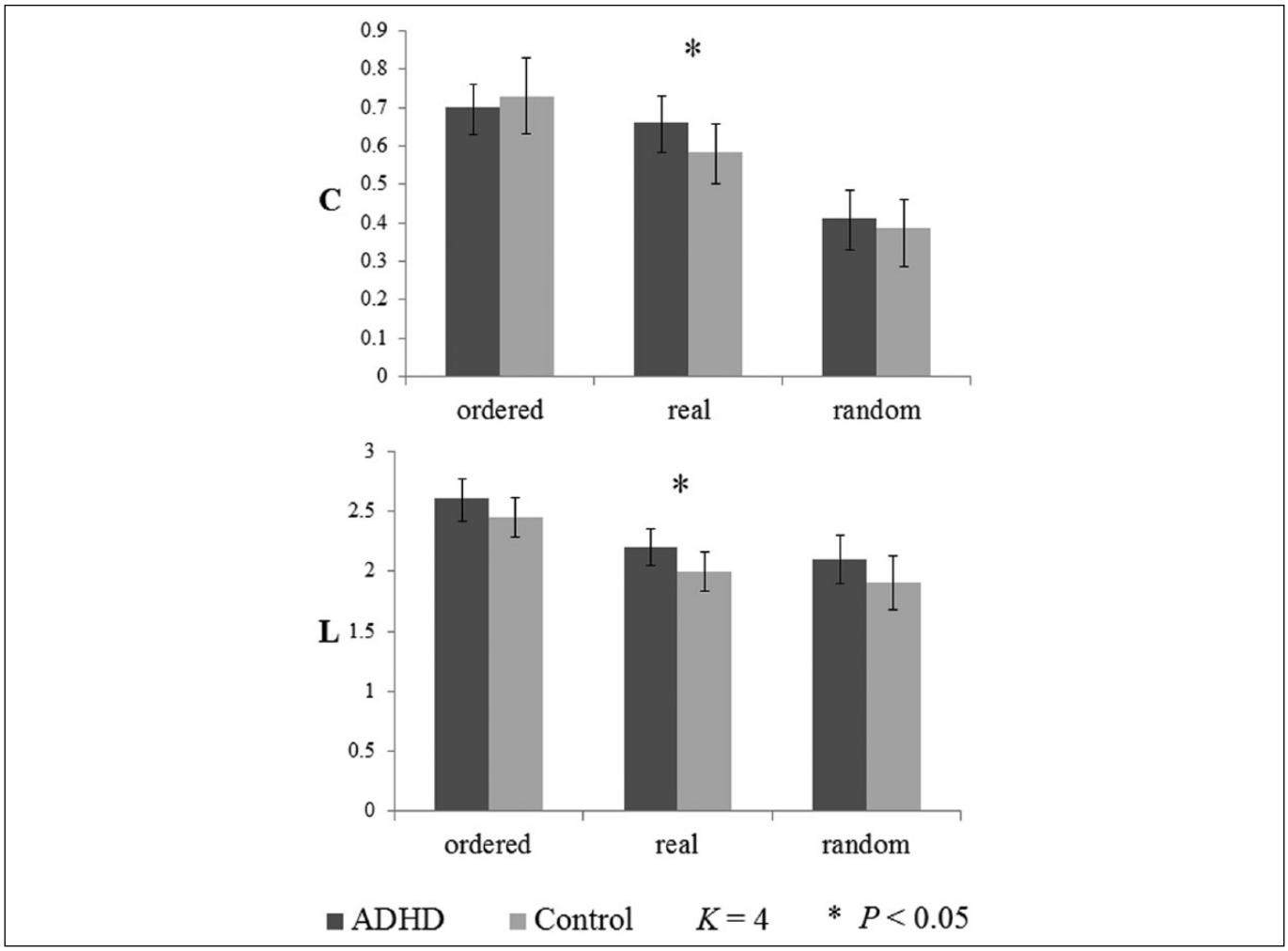

Figure 4. Comparison of *C* and *L* of real networks with those of the constructed random and ordered networks that preserved the degree sequences of their experimental counterparts at *K* = 4 in the beta band. Asterisks indicate significant differences between the 2 groups (*P* < .05).

γ value and decreased λ value in ADHD (compared with normals).

An ordered network has high *C* and *L* values. We found that both *C* and *L* were greater in ADHD than normals (Figure 4). Because the control group's network is small-world, the network of the ADHD group led to a shift of the topologic structure towards an ordered network. The small-world structure reflects the optimal balance between local information processing and global integration. The brain network anomaly of a transformation to a random or ordered network, caused by a brain disorder, reflected a less optimal organizational structure. Although the biologic mechanism of this transformation remains unclear, the structure of the ordered network has been shown to have lower global coordination and slower flow of information than the structure of the small-world network.[28,29]

The correlations between EEG network topologic features (*C* and *L*) in beta and clinical symptoms, or task performance, were also assessed in this study. *DSM*-IV scores of all subjects, including ADHD and normals, were positively correlated with the cluster coefficient. Because *DSM*-IV scores reflect the level of ADHD, a higher score indicates more symptoms of ADHD. Hence, the results indicate that the more symptoms, the more local short connections might appear in beta during MSIT performance. Furthermore, we also found that RT was significantly positively correlated with the cluster coefficient for ADHD, but not for controls. Previous results demonstrated that children with ADHD were significantly slower to react during performance of the MSIT, and *C* in ADHD was significantly higher than that in controls in beta. Increased local characteristics might reflect a compensatory mechanism to inhibit the impact of the disorder on brain networks, which means that the whole brain function integration ability in ADHD was reduced, and the information transfer between different parts of the brain in ADHD was slower than that in normals during MSIT performance. Based on these results, we infer that enhanced local characteristics might cause increased RT in ADHD. We also found that the RTs of the 2 groups were initially not significantly different, but were prolonged in ADHD as the

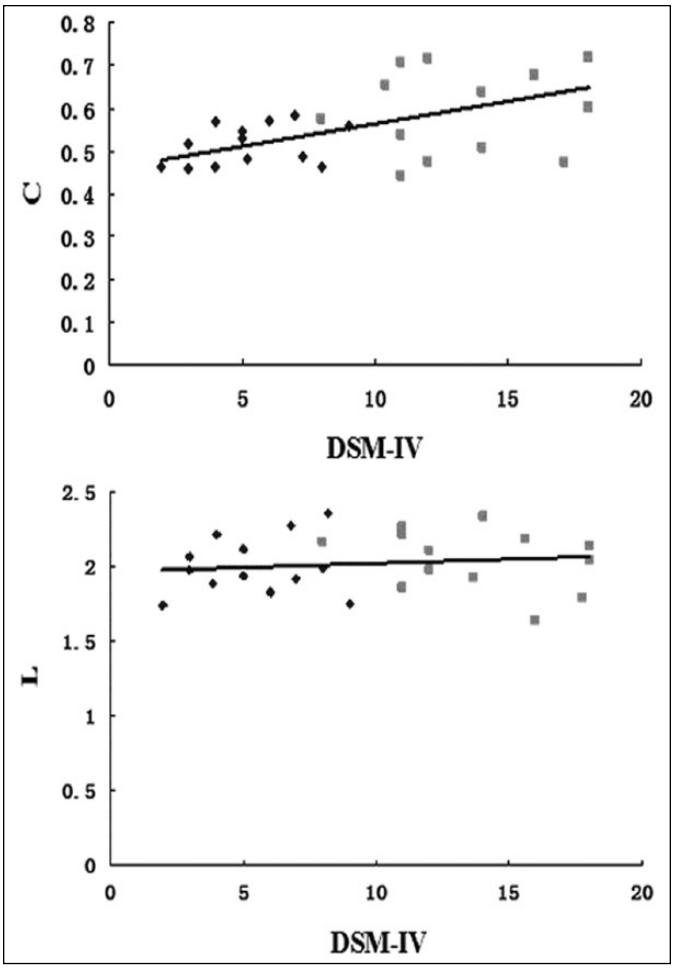

Figure 5. Correlation analyses between *DSM*-IV scores and the network topologic features (*C* and *L*) in the beta band for the ADHD group (squares) and the normal control group (diamonds).

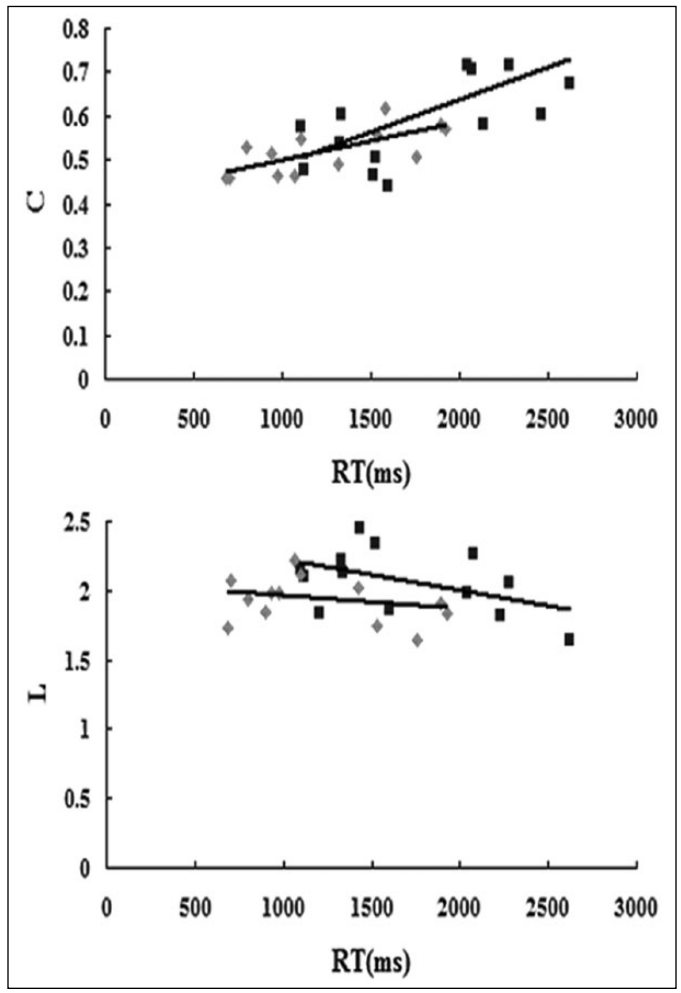

Figure 6. Correlation analyses between RT and the network topologic features (*C* and *L*) in the beta band for the ADHD group (squares) and the normal control group (diamonds).

trials continued. Thus, in future studies, it will be important to investigate, and compare, the relationship between the RTs of subjects with ADHD in early and late trials and their corresponding *C* values, which will contribute to further revealing whether the brain network of ADHD is related to attention.

Conclusions

The results of the present study reveal a wide range of distribution changes in brain attention functional networks, and in the topologic structure of the brain attention functional networks (which transformed to ordered networks), for children with ADHD in the beta band. In addition, they suggest, in beta, that *C* may be positively correlated with *DSM*-IV score, and that the correlation between RT and *C* was significant for the ADHD group on MSIT performance. These findings, which are consistent with those of previous ADHD studies using structural and functional imaging, lend themselves to an interpretation of the disorganization of neural networks in this illness and provide further understanding of the relationship between ADHD and cerebral dysfunction.

Appendix

The degree *K* is a statistical property, which describes the connected vertices. The degree of a vertex is defined as the number of edges between the vertex and other vertices of the network. A vertex with a larger *K* value describes a vertex with a greater number of edges and indicates that the vertex is more important in the network. The degree *K* of the graph is the average number of edges per vertex.

The clustering coefficient *C*, which is an important statistical feature of complex networks, is a measure of the network group level (i.e., local structure). It represents the likelihood that neighbors of a vertex will be connected to each other. The clustering coefficient of the entire network is computed as follows:

$$C = \frac{1}{n}\sum_{i\in N} C_i = \frac{1}{n}\sum_{i\in N}\frac{2t_i}{k_i(k_i-1)}. \tag{1}$$

If one assumes that vertices i are connected to other k_i vertices, there may be up to $k_i(k_i - 1)/2$ edges between the k_i vertices, and t_i edges actually exist, so the clustering coefficient of

node i is C_i. Note that n is the number of vertices in the graph N. The range of C is between 0 and 1.

The characteristic path length L plays an important role in the transmission of information in a network. It is a global characteristic that describes the network's internal structure and indicates how well integrated the network is. The network characteristic path length L is the average shortest path connecting any 2 vertices of the graph and is defined as follows:

$$L = \frac{1}{n}\sum_{i\in N} L_i = \frac{1}{n}\sum_{i\in N}\frac{\sum_{j\in N, j\neq i} d_{ij}}{n-1}. \quad (2)$$

Note that d_{ij} is the connection distance between any 2 vertices i and j, which is defined as the shortest path to connect 2 vertices. The shortest path d_{ij} characterizes the optimal path of information from one vertex to reach another vertex in the network, by which the network can transmit information faster. L_i is the average distance from vertex i to all other vertices, and n is the number of vertices in the graph N. The range of L is also between 0 and 1.

Acknowledgment

We thank the 2 anonymous reviewers for their constructive comments.

Declaration of Conflicting Interests

The author(s) declared no conflicts of interest with respect to the research, authorship, and/or publication of this article.

Funding

The author(s) disclosed receipt of the following financial support for the research, authorship, and/or publication of this article: grant 81071150 from the National Natural Science Foundation of China and grant 2008B09050023 from the Produce-Study-Research program, Guangdong Province, Ministry of Education of China.

References

1. Bush G. Attention-deficit/hyperactivity disorder and attention networks. *Neuropsychopharmacology* 2010;35(1):278–300.
2. Biederman J, Faraone SV. Attention-deficit hyperactivity disorder. *Lancet*. 2005;366(9481):237–248.
3. Hill DE, Yeo RA, Campbell RA, Hart B, Vigil J, Brooks W. Magnetic resonance imaging correlates of attention-deficit/hyperactivity disorder in children. *Neuropsychology*. 2003;17(3):496–506.
4. Makris N, Buka SL, Biederman J, et al. Attention and executive systems abnormalities in adults with childhood ADHD: a DT-MRI study of connections. *Cereb Cortex*. 2008;18(5):1210–1220.
5. Vance A, Silk TJ, Casey M, et al. Right parietal dysfunction in children with attention deficit hyperactivity disorder, combined type: a functional MRI study. *Mol Psychiatry*. 2007;12(9):826–832.
6. Smith AB, Taylor E, Brammer M, Halari R, Rubia K. Reduced activation in right lateral prefrontal cortex and anterior cingulate gyrus in medication-naïve adolescents with attention deficit hyperactivity disorder during time discrimination. *J Child Psychol Psychiatry*. 2008;49(9):977–985.
7. Watts DJ, Strogatz SH. Collective dynamics of "small-world" networks. *Nature*. 1998;393:440–442.
8. Stam CJ, Van Straaten ECW. The organization of physiological brain networks. *Clin Neurophysiol*. 2012;123(6):1067–1087.
9. Fallani FDV, Astolfi L, Cincotti F, et al. Cortical functional connectivity networks in normal and spinal cord injured patients: evaluation by graph analysis. *Hum Brain Mapp*. 2007;28(12):1334–1346.
10. Stam CJ, Jones BF, Nolte G, Breakspear M, Scheltens P. Small-world networks and functional connectivity in Alzheimer's disease. *Cereb Cortex*. 2007;17(1):92–99.
11. Ponten SC, Bartolomei F, Stam CJ. Small-world networks and epilepsy: graph theoretical analysis of intracerebrally recorded mesial temporal lobe seizures. *Clin Neurophysiol*. 2007;118(4):918–927.
12. Liu Y, Liang M, Zhou Y, et al. Disrupted small-world networks in schizophrenia. *Brain*. 2008;131(4):945–961.
13. Wang H, Douw L, Hernández JM, Reijneveld JC, Stam CJ, Van Mieghem P. Effect of tumor resection on the characteristics of functional brain networks. *Phys Rev E*. 2010;82(2):021924.
14. Wang L, Zhu CZ, He Y, et al. Altered small-world brain functional networks in children with attention-deficit/hyperactivity disorder. *Hum Brain Mapp*. 2009;30(2):638–649.
15. Ahmadlou M, Adeli H, Adeli A. Graph theoretical analysis of organization of functional brain networks in ADHD. *Clin EEG Neurosci*. 2012;43(1):5–13.
16. Bush G, Shin LM. The Multi-Source Interference Task: an fMRI task that reliably activates the cingulo-frontal-parietal cognitive/attention network in individual subjects. *Nat Protoc*. 2006;1:308–313.
17. Stam CJ, Van Dijk BW. Synchronization likelihood: an unbiased measure of generalized synchronization in multivariate data sets. *Physica D*. 2002;163(3–4):236–241.
18. Conners CK, Sitarenios G, Parker JDA, Epstein JN. The Revised Conners' Parent Rating Scale (CPRS-R): factor structure, reliability, and criterion validity. *J Abnorm Child Psychol*. 1998;26(4):257–268.
19. DuPaul GJ, Power TJ, Anastopoulos AD, Reid R, eds. *ADHD Rating Scale IV: Checklists Norms & Clinical Interpretation*. New York: Guilford; 1998.
20. van Dongen-Boomsma M, Lansbergen MM, Bekker EM, et al. Relation between resting EEG to cognitive performance and clinical symptoms in adults with attention-deficit/hyperactivity disorder. *Neurosci Lett*. 2010;469(1):102–106.
21. Lahey BB, Pelham WE, Stein MA, et al. Validity of *DSM*-IV attention-deficit/hyperactivity disorder for younger children. *J Am Acad Child Adolesc Psychiatry*. 1998;37(7):695–702.
22. Stroop JR. Studies of interference in serial verbal reactions. *J Exp Psychol*. 1935;18:643–662.
23. Eriksen BA, Eriksen CW. Effects of noise letters upon the identification of a target letter in a nonsearch task. *Percept Psychophys*. 1974;16(1):143–149.
24. Shen M, Sun L, Chan F. Method for extracting time-varying rhythms of electroencephalography via wavelet packet analysis. *IEEE Proc Sci Meas Technol*. 2001;148(1):23–27.
25. Milo R, Shen-Orr S, Itzkovitz S, Kashtan N, Chklovskii D, Alon U. Network motifs: simple building blocks of complex networks. *Science*. 2002;298(5594):824–827.
26. Backs RW, Boucsein W, eds. *Engineering Psychophysiology: Issues and Applications*. Hillsdale, NJ: Lawrence Erlbaum; 2000:241–253.
27. Latora V, Marchiori M. Efficient behavior of small-world networks. *Phys Rev Lett*. 2001;87(19):198701.
28. Barahona M, Pecora LM. Synchronization in small-world systems. *Phys Rev Lett*. 2002;89(5):054101.
29. Nishikawa T, Motter AE, Lai YC, Hoppensteadt FC. Heterogeneity in oscillator networks: are smaller worlds easier to synchronize? *Phys Rev Lett*. 2003;91(1):014101.